Side Chain Influence on the Mass Density and Refractive Index of Polyfluorenes and Star-Shaped Oligofluorene Truxenes

Paulina O. Morawska[1], Yue Wang[1†], Arvydas Ruseckas[1], Clara Orofino-Peña[2], Alexander L. Kanibolotsky[2#], Ramkumar Santhanagopal[3], Nils Fröhlich[3], Martin Fritsch[3], Sybille Allard[3], Ullrich Scherf[3], Peter J. Skabara[2], Ifor. D.W. Samuel[1], Graham A. Turnbull[1]

1. Organic Semiconductor Centre, SUPA, School of Physics and Astronomy, University of St Andrews, North Haugh, St Andrews KY16 9SS (UK)

2. WestCHEM, Department of Pure and Applied Chemistry, University of Strathclyde, 295 Cathedral Street, Glasgow G1 1XL, UK

3. Chemistry Department and Institute for Polymer Technology, Wuppertal University, Gauss-Str. 20, D-42119 Wuppertal, Germany

Abstract

The density of organic semiconductor films is an important quantity because it is related to intermolecular spacing which in turn determines the electronic and photophysical properties. We report thin film density and refractive index measurements of polyfluorenes and star-shaped oligofluorene truxene molecules. An ellipsometer and a procedure using a spectrophotometer were used to determine film thickness and mass of spin-coated films, respectively. We present a study of the effect of alkyl side chain length on the volumetric mass density and refractive index of the materials studied. The density measured for poly(9,9-di-n-octylfluorene) (PF8) was 0.88 ± 0.04 g/cm^3 and decreased with longer alkyl side chains. For the truxene molecule with butyl side chains (T3 butyl), we measured a density of 0.90 ± 0.04 g/cm^3, which also decreased with increasing side-chain length.

Introduction

Thin films of organic semiconductors are used in a wide range of optoelectronic applications including photovoltaic devices [1,2], OLEDs [3,4], transistors [5], distributed feedback lasers [6,7,8], biological and chemical sensors [9,10,11]. Their widespread use has benefitted from their tunable their photonic and electronic properties, which can be tailored by various methods including addition of substituents to the main core of the molecule[12,13,14], molecular engineering of the band gaps[15], control of morphology to extend conjugation length[16,17], and control of film thickness[18]. The resulting materials properties in the solid-state depend not only on the electronic properties of individual molecules but also on the density of the film, i.e. how closely the molecules pack together [19]. For instance, porphyrin-cored conjugated dendrimers showed dependence of the photoluminescence quantum yield (PLQY) on core – core interactions with various rings attached [20]. Charge transport also depends strongly on the intermolecular spacing as charges have to hop between molecules. The hopping process is strongly dependent on the intermolecular overlap of neighbouring molecules, and so also on the density of the molecules [21,22]. Additionally, the density of molecules affects other important processes including exciton diffusion involved in highly efficient photovoltaic devices [17].

There is growing interest in measuring the microscopic morphology of the film using X-ray diffraction, atomic force microscopy, neutron scattering, and scanning electron microscopy but there are surprisingly few published measurements of film density. Methods reported in the literature to study the density of thin films include the pressure-of-flotation method [23], X-ray reflectivity [24], selected-area electron diffraction combined with X-ray diffraction [25], and the solution absorbance method [26]. In the pressure-of-flotation method the density is obtained by measuring the relative density difference and mass difference between a clean substrate

and a substrate coated with the film. The relative density difference is found by applying pressure to a working liquid in which the test sample is placed, until the density of the liquid is in equilibrium with the density of the test sample. This method requires complex and sensitive apparatus to measure density values. The XRR and XRD methods analyse the reflected or diffracted beam from a very thin sample as a function of the angles of incidence and detection. These methods can be used for density measurements of materials possessing crystalline structure but not of amorphous films. In the solution absorbance technique [26] the thickness of a thin evaporated molecular film is measured with a surface profilometer and then the film is dissolved in a solvent. The absorbance of the resulting solution is compared against standards of the same material to determine the mass. The method is simple but has some limitations in its application to soft materials, such as solution processed conjugated polymers, since the surface profilometer can be inaccurate or even damage very thin polymer films.

In this paper we present density measurements of two families of fluorene-based organic semiconductors: long chain polyfluorenes and star-shaped oligodialkylfluorene truxenes. Polyfluorenes are well established printable OLED materials, while their star-shaped analogues have been reported as low threshold, tuneable laser materials [13,27,18,28,29]. To measure the density of the spin-coated films we used an improved solution absorbance method. In this improved method we first removed the edge bead from the spin-coated films to give samples of uniform thickness, and used spectroscopic ellipsometry to measure thickness with higher accuracy. We investigate the effect of alkyl side chain length on the volumetric mass density and refractive index for both fluorene families.

Experimental

The chemical structures of the polyfluorenes (PF) and oligofluorene truxenes (T3) studied in this paper are shown in Figure 1. The polyfluorene repeat units have either dioctyl (PF8), didodecyl (PF12) or dipentadecyl (PF15) alkyl side chains attached to the methylene bridge (Figure 1a), these polymers being synthesied according to the procedures in references [30,31,32,33]. The star-shaped T3 molecules consist of a central truxene core with three terfluorene arms (Figure 1b). Both the core and arms contain either butyl (T3 butyl) , hexyl (T3 hexyl) or octyl (T3 octyl) side chain substituents. The general synthesis of the T3 molecules can be found in reference [28]. The molecular weights of the truxene molecules and of the polymer repeat units are presented in table 1.

Material	Molecular weight of molecules or repeat unit of polymer [g/mol]
T3 butyl	3167
T3 hexyl	3840
T3 octyl	4513
PF8	389
PF12	501
PF15	585

Table 1. Molecular weights of the truxenes molecules and of the polyfluorene polymer repeat units

Absorption spectra were measured with a Cary 300 UV-Vis spectrophotometer. Fluorescence spectra were measured with a Jobin Yvon FluoroMax2. Values of absolute photoluminescence quantum yield (PLQY) of approximately 50 nm thick films were

measured using an integrating sphere [34] in a Hamamatsu Photonics C9920-02 system with continuous excitation at 355 nm by a monochromated Xenon lamp.

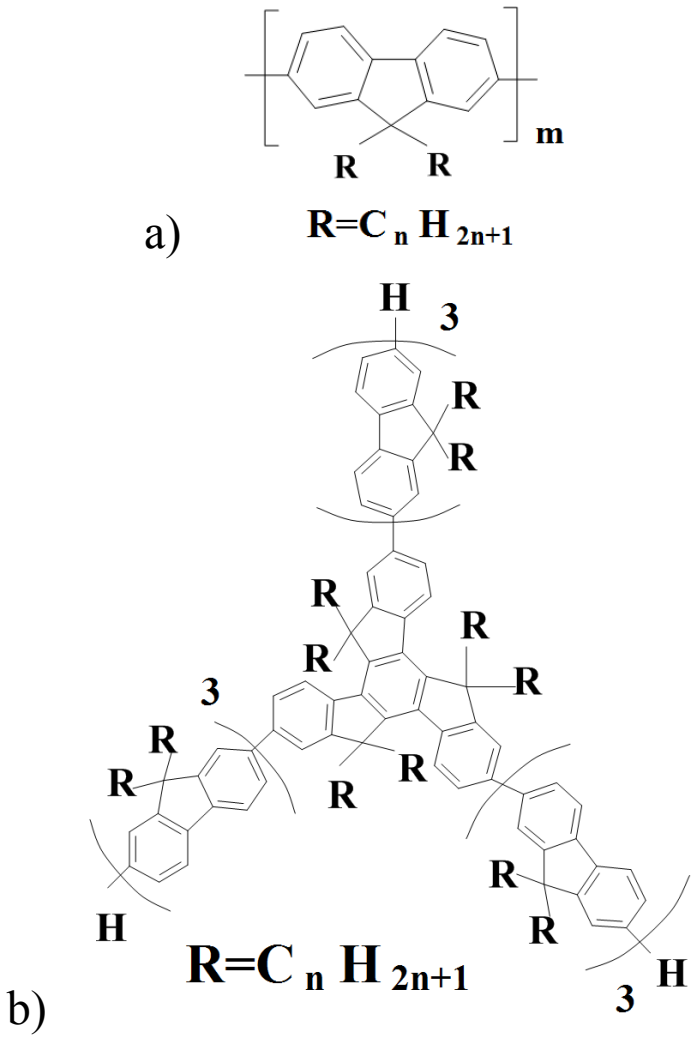

Figure 1. Chemical structure of the molecules used in the studies. 1a) di-alkyl polyfluorene, where the side chains consist of n=8, 12, or 15 carbon atoms; 1b) tris(terfluorenyl)truxene, where the side chains consist of n = 4, 6, or 8 carbon atoms

Samples for the density measurements were prepared on 15 mm × 15 mm silicon substrates. These were first cleaned by ultrasonification in acetone and isopropanol solvents for 10 min each. Next, the substrates were treated in an oxygen plasma asher for 3 min. Films were deposited by spin-coating from chlorobenzene (for polyfluorenes) and toluene (for truxenes)

solutions on the pre-prepared silicon wafers. The solution concentrations used were 15 mg/ml for PF8 and PF12, 7.5 mg/ml for PF15, and 12 mg/ml for all the truxene materials. For each material we fabricated four samples. To ensure that the films used in the experiment were of a uniform thickness across the whole substrate, a square section of area 10 mm × 10 mm was cleaved from the center of a bigger substrate. The dimension of each cleaved substrate was accurately measured with calipers. The area of each piece of silicon wafer was measured by averaging five measurements of x and y substrate sides. The film thickness and refractive index were then measured by variable angle spectroscopic ellipsometry (J.A. Woollam Co. Inc. M2000-DI). This contactless measurement is based on determining changes in the polarization state of light reflected from the thin film. The spectroscopic range of the collected data was 190 nm – 1700 nm and the measurements were performed for incidence angles 45° – 75° in steps of 5°. To evaluate film thickness from the recorded data, a Cauchy model was fitted in the transparent range (between 480 nm – 1700 nm) for four samples of each material. The film thicknesses were measured to be in the range of 55 – 75 nm for all samples.

To calculate the molar density of each sample, we used the film thickness obtained from ellipsometry and determined the mass of the films using an absorption measurement recorded in the spectral range 300 nm – 480 nm. We first measured the absorbance of a 3 ml reference solution with known mass of the dissolved material which was prepared from a stock solution of higher concentration. The film samples were then each placed in a quartz cuvette (10 mm path length) filled with 3 ml of the same solvent used for spin-coating. We measured the optical density of each dissolved sample, as depicted in Figure 2. The mass was calculated from (1):

$$m = \frac{a_1}{a_2} m_{ref}, \qquad (1)\ ,$$

where m is mass of the film, a_1 is the spectrally integrated absorbance measured for the dissolved film, a_2 is the integrated absorbance measured for the reference sample and m_{ref} is the known mass of the solute in the reference solution. Care was taken to ensure that the film was fully dissolved prior to the absorbance measurement, and after the measurement the substrate was inspected in a fluorescence measurement to validate that the film had been completely removed.

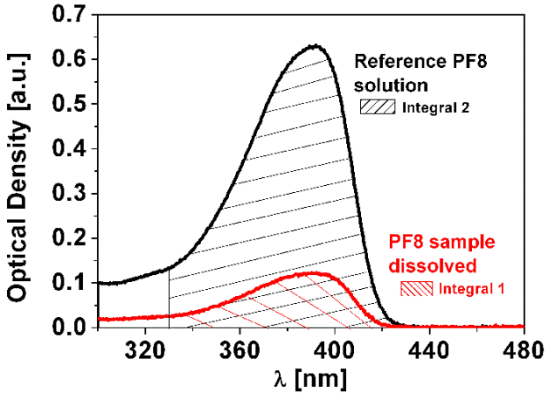

Figure 2. Absorption spectra of a PF8 sample dissolved in 3 ml of solvent and PF8 reference solution. The integral under the absorbance curve was used to calculate the mass of the polymer film.

The mass density ρ was than calculated from (2):

$$\rho = \frac{m}{V} = \frac{m}{dxy}, \qquad (2)\ ,$$

where d is the thickness of the film and x and y are the length and width of the substrate, respectively.

Results and discussion:

Figure 3 shows the absorption and photoluminescence (PL) spectra of films of the polyfluorenes (Figure 3a) and truxenes (Figure 3b). The excitation wavelengths used were 355 nm for the polyfluorenes and 325 nm for the truxenes. The absorption maxima and main

emission peaks for each family are presented in table 2. The peak absorption wavelengths in polyfluorenes and truxenes do not change much between the members of each family. We observe a few nanometres spectral shift of the absorption peak towards longer wavelengths with an increase of the side chain length for both families. The absorption shifts may be caused by a change in solid-state packing, with reduced aggregation or increasing backbone coplanarity for increasing side chain length, possibly driven by hydrophobic side-chain interactions. The red-shift is less pronounced for the truxenes series, with the conjugation length limited by the fixed arm length. The absorbance per unit film thickness is shown in Figure 3. We observe that the thickness-normalized absorbance increases for polyfluorenes with longer side chains (consistent with an increase in transition dipole), while it has a maximum for the oligofluorene truxene with hexyl side chains.

The PL spectra are very similar for all the truxenes but there is a noticeable red-shift in the PL spectrum of PF12. The red-shifted PL signature for PF12 may indicate an increased geometrical reorganization in PF for C12 side chains. Film PLQY measurements were performed using an excitation wavelength of 325 nm for truxenes and 355 nm for polyfluorenes. The solid-state PLQYs were measured in a nitrogen atmosphere and the results are presented in Table 2. The uncertainty of the PLQY measurement is ± 2%. The PLQYs do not show a clear trend with increasing side chain length, although the molecules with the shortest side chains in each family exhibit the lowest PLQY.

Material	Peak absorption wavelength [nm]	PL peak wavelengths [nm]	PLQY [%]
PF 8	386	423, 445	36
PF12	392	432, 456	54
PF15	395	422, 446	40
T3butyl	364	413, 437	63
T3hexl	367	412, 435	83
T3octyl	368	412, 435	80

Table 2. PLQY and peak wavelengths of the thin films absorption and PL spectra of polyfluorenes and oligofluorene truxenes

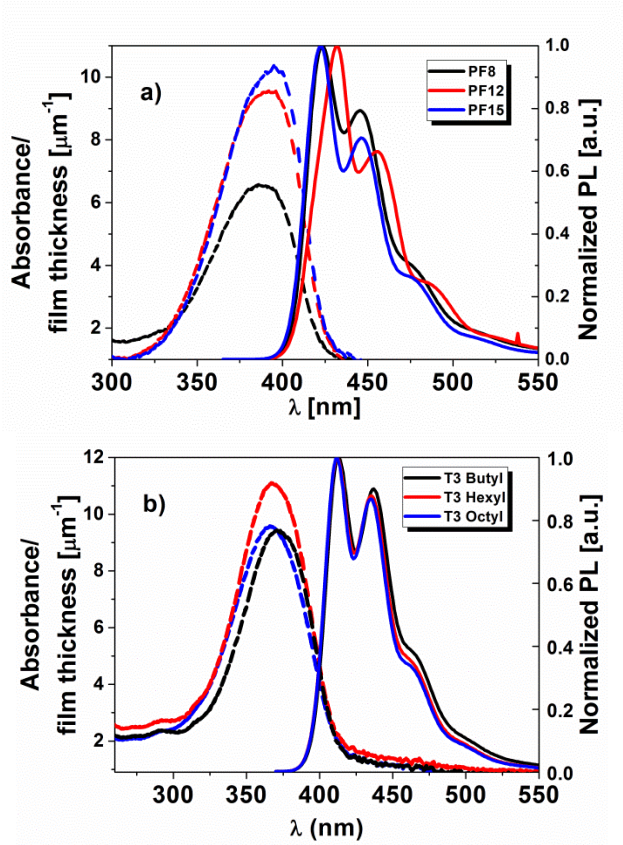

Figure 3a) Absorption (dashed line) and fluorescence (solid line) spectra of the polyfluorene films. Figure 3b) Absorption and fluorescence spectra of truxene films.

To determine film thickness the ellipsometry data was fitted with an isotropic refractive index model. This choice of model is reasonable as truxene molecules have previously been reported to arrange with random orientations [18], while polymers with low molecular weight also tend towards an isotropic molecular arrangement as shown by Koynov *et al.* [35]. For the particular polymers in this study we also tried to fit with an anisotropic model but found the best fitting was for the isotropic model. The fitting mean squared error (MSE) values for all materials were in the range 0.62 – 1.20 indicating that the ellipsometric model fits very well to the obtained data. The measured film thicknesses for polyfluorenes were in the range 60 – 75 nm and 55 – 60 nm for truxenes.

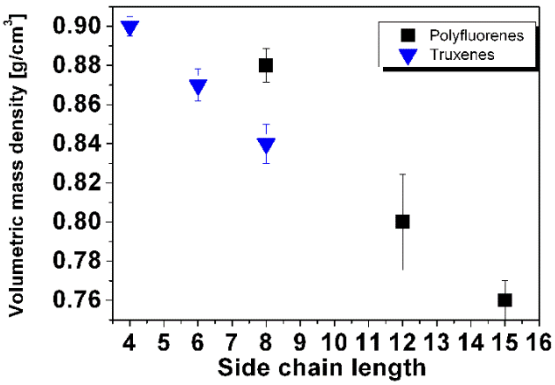

Figure 4. Mass density obtained for polyfluorenes (black squares) and truxenes (blue triangles) as a function of the number of carbon atoms in the alkyl side chains.

Figure 4 presents the film density dependence on the side chain length of the polymer or truxene molecules in this study. The density of PF8 is (0.88 ± 0.04) g/cm^3, and of T3 butyl is (0.90 ± 0.04) g/cm^3. For both polyfluorenes and truxenes, the density decreases with an increase of the side chain length. The rate of change in density with side chain length is approximately the same for both sets of materials. For octyl side chains we find that the density is lower for the star-shaped molecules (T3 octyl) than for the polymer (PF8). The lower density of the truxene could arise from its greater rigidity and the star-shape motif

inhibiting dense packing. Using the molecular weight and density of the material, we calculated the average spacing of the truxene molecules, as shown in Table 3. From these results we estimate that an increase of the side chain length by two carbon atoms causes approximately an 8% increase in average spacing of the truxene cores.

Material	Density [g/cm^3]	Volume / Molecule [nm^3]	Mean spacing (1D) [nm]
T3 butyl	0.90	5.84	1.8
T3 hexyl	0.87	7.33	1.94
T3 octyl	0.84	8.92	2.07

Table 3. Average molecular volume and molecular spacing of the truxene molecules in thin films

To benchmark the values of densities obtained, we repeated the measurement for the organic semiconductor 4,4'-N,N'-dicarbazole-biphenyl (CBP), for which the film density was previously reported [26]. The density of our spin-coated CBP film was found to be (1.08 ± 0.04) g/cm^3, whereas the Lai group has reported that the density of CBP for an evaporated film was (1.18 ± 0.02) g/cm^3. The small difference between the two values could be explained by the different methods of film fabrication. During evaporation, the molecules have more time to arrange in a closely packed film than for the faster process of spin-coating where the conformation is kinetically frozen when the solvent evaporates. Closer packing of molecules will give a higher density of the film. This result is consistent with higher refractive index data measured for evaporated films [36,37]**.** It is possible that residual solvent in the spin-cast films may reduce the chromophore density [38]**.** To test if this may affect our results we measured the thickness of a PF8 film immediately after spin-casting and again after a period of 2 hours under a vacuum of 10^{-4} mb. The film thickness before and after prolonged vacuum exposure were 73 nm and 72 nm. We therefore conclude that any residual solvent effects are negligible in these rigid chain materials to the densities measured.

We have also evaluated the density of poly[9,9'-(2-d_{17} –ethylhexyl)fluorene] (PF26) based on neutron reflectivity results [39]. The scattering length density (SLD) is defined as:

$$\text{SLD} = \frac{\rho N_A \sum_i b_i}{M}, \quad (3)$$

where ρ is film density, $N_A$is the Avogadro number, b_i is the coherent scattering length of all nuclei and M is the molecular weight of the repeat unit. The SLD reported for PF26 at room temperature was $5.0 \pm 0.1 \times 10^{-6}$ Å^{-2} and using the coherent scattering lengths: b_C = 6.65 fm, b_H =-3.74 fm and b_D=6.67 fm for carbon, hydrogen and deuterium, respectively, we obtain a PF26 film density of 0.88 g/cm^3. As the PF26 molecular structure is very similar to the PF8 chemical structure, we expect that they would have similar film density.

From the ellipsometry data we also extracted the wavelength dependence of the refractive index across the spectral range 400-800 nm of each material, as shown in Figure 5. The refractive indices of the T3-butyl, T3-hexyl and T3-octyl reduce systematically with increasing side chain length (Figure 5a). The polyfluorenes (Figure 5b) show the same trend for longer wavelengths (in the transparent range of the materials). Figure 5c compares the refractive indices for both families at 800 nm, far from the absorption edge. The refractive index shows the same trend as the density in Figure 4, where the molecules with shorter side chains have a higher refractive index in the transparent range. The refractive index of the films is therefore strongly dependent on the density of the conjugated chromophores.

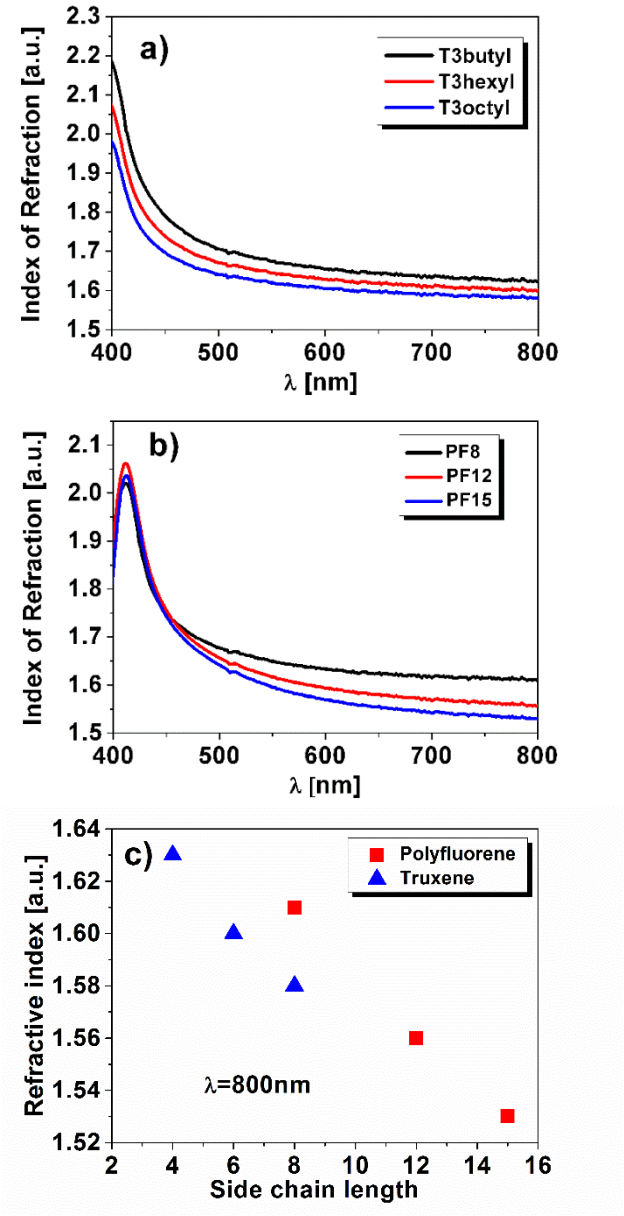

Figure 5 a) the refractive index measured by spectroscopic ellipsometry of the oligofluorene truxenes; b) the refractive index of polyfluorenes; c) the refractive index dependence on side chain length for truxene molecules and polyfluorenes, measured at a wavelength of 800 nm.

The relationship between film density, absorption and photoluminescence in these families of molecules is more complex, as the less dense polymers show stronger, red-shifted absorption. This indicates that the side chain length affects the transition strength of the chromophores as

well as their number density. The combination of these two effects is apparent in Figure 5b where at short wavelengths close to the absorption edge of the polyfluorenes, the PF8 refractive index curve is found to cross over the other curves. This crossing close to the absorption resonance may be related to the broader, weaker absorption of the PF8, compared with the other two polymers. While the densest films of each family exhibit the lowest PLQY, other changes in PL properties do not clearly correlate with film density, and so may be influenced by local variations in both chromophore conformation and packing.

Conclusion

We have presented a detailed investigation of the effect alkyl side chain on the molecular density and refractive index of polyfluorenes and oligofluorene truxenes. We have used an improved solution absorbance method to determine densities of films spin-coated from small molecules and polymers. We observe that the densities of both families decrease with increasing length of alkyl sides chains, and find that their refractive indices correlate with variations in density.

Corresponding Authors

Prof Graham Turnbull gat@st-andrews.ac.uk Prof Ifor Samuel idws@st-andrews.ac.uk

Present Addresses

† Department of Physics, University of York, Heslington, York, YO10 5DD, UK

Institute of Physical-Organic Chemistry and Coal Chemistry, 02160 Kyiv, Ukraine

Funding Sources

TIRAMISU (FP7/2007-2013) under grant agreement n◦284747

EPSRC grants EP/J009016/1, EP/F059922/1

Acknowledgment

This work is part of the TIRAMISU project, funded by the European Commission's Seventh Framework Programme (FP7/2007-2013) under grant agreement n◦284747, and the *Engineering and Physical Sciences Research Council* (*EPSRC*) grants EP/J009016/1 and EP/F059922/1. The authors would like to acknowledge Dr Gordon Hedley for helpful discussions during this work. I.D.W.S. and P.J.S. are Royal Society Wolfson Research Merit Award holders.

References:

(1) Shaheen, S. E.; Brabec, C. J.; Sariciftci, N. S.; Padinger, F.; Fromherz, T.; Hummelen, J. C. 2.5% Efficient Organic Plastic Solar Cells. *Appl Phys Lett* **2001**, *78* (6), 841–843.

(2) Scharber, M. C.; Sariciftci, N. S. Efficiency of Bulk-Heterojunction Organic Solar Cells. *Progress in Polymer Science*. 2013, pp 1929–1940.

(3) Zhang, S.; Turnbull, G. A.; Samuel, I. D. W. Highly Efficient Solution-Processable Europium-Complex Based Organic Light-Emitting Diodes. *Organic Electronics*. 2012, pp 3091–3096.

(4) Zhang, S.; Turnbull, G. A.; Samuel, I. D. W. Enhancing the Emission Directionality of Organic Light-Emitting Diodes by Using Photonic Microstructures. *Appl. Phys. Lett.* **2013**, *103* (21).

(5) Muccini, M. A Bright Future for Organic Field-Effect Transistors. *Nat. Mater.* **2006**, *5* (8), 605–613.

(6) Turnbull, G. A.; Andrew, P.; Jory, M. J.; Barnes, W. L.; Samuel, I. D. W. Emission Characteristics and Photonic Band Structure of Microstructured Polymer Lasers. In *Synthetic Metals*; 2002; Vol. 127, pp 45–48.

(7) Vasdekis, A. E.; Tsiminis, G.; Ribierre, J.-C.; O' Faolain, L.; Krauss, T. F.; Turnbull, G. A.; Samuel, I. D. W. Diode Pumped Distributed Bragg Reflector Lasers Based on a Dye-to-Polymer Energy Transfer Blend. *Opt. Express* **2006**, *14* (20), 9211–9216.

(8) Yang, Y.; Turnbull, G. A.; Samuel, D. W. Sensitive Explosive Vapor Detection with Polyfluorene Lasers. *Adv. Funct. Mater.* **2010**, *20* (13), 2093–2097.

(9) Yang, J.; Swager, T. M. Fluorescent Porous Polymer Films as TNT Chemosensors : Electronic and Structural Effects Fluorescent Porous Polymer Films as TNT Chemosensors : Electronic and Structural Effects. **1998**, No. 4, 11864–11873.

(10) Rose, A.; Zhu, Z.; Madigan, C. F.; Swager, T. M.; Bulović, V. Sensitivity Gains in Chemosensing by Lasing Action in Organic Polymers. *Nature* **2005**, *434* (7035), 876–879.

(11) Haughey, A.-M.; Guilhabert, B.; L Kanibolotsky, A.; J Skabara, P.; D Dawson, M.; A Burley, G.; Laurand, N. An Oligofluorene Truxene Based Distributed Feedback Laser for Biosensing Applications. *Biosens. Bioelectron.* **2013**, *54C*, 679–686.

(12) Misra, R.; Jadhav, T.; Mobin, S. M. Aryl Pyrazaboles: A New Class of Tunable and Highly Fluorescent Materials. *Dalt. Trans.* **2013**, *42* (47), 16614–16620.

(13) Misra, R.; Sharma, R.; Mobin, S. M. Star Shaped Ferrocenyl Truxenes: Synthesis, Structure and Properties. *Dalton Trans.* **2014**, 6891–6896.

(14) Bright, D. W.; Dias, F. B.; Galbrecht, F.; Scherf, U.; Monkman, A. P. The Influence of Alkyl-Chain Length on Beta-Phase Formation in Polyfluorenes. *Adv. Funct. Mater.* **2009**, *19* (1), 67–73.

(15) Roncali, J. Molecular Engineering of the Band Gap of Π-Conjugated Systems: Facing Technological Applications. *Macromol. Rapid Commun.* **2007**, *28* (17), 1761–1775.

(16) Peet, J.; Brocker, E.; Xu, Y.; Bazan, G. C. Controlled β-Phase Formation in poly(9,9-Di-N-Octylfluorene) by Processing with Alkyl Additives. *Adv. Mater.* **2008**, *20* (10), 1882–1885.

(17) Hedley, G. J.; Ward, A. J.; Alekseev, A.; Howells, C. T.; Martins, E. R.; Serrano, L. A; Cooke, G.; Ruseckas, A.; Samuel, I. D. W. Determining the Optimum Morphology in High-Performance Polymer-Fullerene Organic Photovoltaic Cells. *Nat. Commun.* **2013**, *4*, 2867.

(18) Wang, Y.; Tsiminis, G.; Yang, Y.; Ruseckas, A.; Kanibolotsky, A. L.; Perepichka, I. F.; Skabara, P. J.; Turnbull, G. a.; Samuel, I. D. W. Broadly Tunable Deep Blue Laser Based on a Star-Shaped Oligofluorene Truxene. *Synth. Met.* **2010**, *160* (13-14), 1397–1400.

(19) Schwartz, B. J. Conjugated Polymers as Molecular Materials: How Chain Conformation and Film Morphology Influence Energy Transfer and Interchain Interactions. *Annu. Rev. Phys. Chem.* **2003**, *54*, 141–172.

(20) Frampton, M. J.; Magennis, S. W.; Pillow, J. N. G.; Burn, P. L.; Samuel, I. D. W. The Effect of Intermolecular Interactions on the Electro-Optical Properties of Porphyrin

Dendrimers with Conjugated Dendrons. *Journal of Materials Chemistry*. 2002, pp 235–242.

(21) Kline, R. J.; McGehee, M. D. Morphology and Charge Transport in Conjugated Polymers. *Polym. Rev.* **2006**, *46* (1), 27–45.

(22) Lupton, J.; Samuel, I.; Beavington, R.; Frampton, M.; Burn, P.; Bässler, H. Control of Mobility in Molecular Organic Semiconductors by Dendrimer Generation. *Physical Review B*. 2001.

(23) Waseda, A.; Fujii, K. Density Evaluation of Silicon Thermal-Oxide Layers on Silicon Crystals by the Pressure-of-Flotation Method. In *IEEE Transactions on Instrumentation and Measurement*; 2007; Vol. 56, pp 628–631.

(24) Schalchli, a; Benattar, J. J.; Licoppe, C. Accurate Measurements of the Density of Thin Silica Films. *Europhys. Lett.* **2007**, *26* (4), 271–276.

(25) Chen, S. H.; Chou, H. L.; Su, A. C.; Chen, S. A. Molecular Packing in Crystalline Poly(9,9-Di- N -Octyl-2,7-Fluorene). *Macromolecules* **2004**, *37* (18), 6833–6838.

(26) Xiang, H. F.; Xu, Z. X.; Roy, V. A. L.; Che, C. M.; Lai, P. T. Method for Measurement of the Density of Thin Films of Small Organic Molecules. *Rev. Sci. Instrum.* **2007**, *78* (3).

(27) Heliotis, G.; Xia, R.; Bradley, D. D. C.; Turnbull, G. A.; Samuel, I. D. W.; Andrew, P.; Barnes, W. L. Blue, Surface-Emitting, Distributed Feedback Polyfluorene Lasers. *Appl. Phys. Lett.* **2003**, *83* (11), 2118–2120.

(28) Kanibolotsky, A. L.; Berridge, R.; Skabara, P. J.; Perepichka, I. F.; Bradley, D. D. C.; Koeberg, M. Synthesis and Properties of Monodisperse Oligofluorene-Funcfionalized Truxenes: Highly Fluorescent Star-Shaped Architectures. *J. Am. Chem. Soc.* **2004**, *126* (42), 13695–13702.

(29) Lai, W. Y.; Xia, R.; He, Q. Y.; Levermore, P. A.; Huang, W.; Bradley, D. D. C. Enhanced Solid-State Luminescence and Low-Threshold Lasing from Starburst Macromolecular Materials. *Adv. Mater.* **2009**, *21* (3), 355–360.

(30) Grell, B. M.; Knoll, W.; Lupo, D.; Meisel, A.; Miteva, T.; Neher, D.; Nothofer, H.; Scherf, U.; Yasuda, A. Blue Polarized Electroluminescence from a Liquid Crystalline Polyfluorene. *Communications* **1999**, 671–675.

(31) Gomulya, W.; Costanzo, G. D.; De Carvalho, E. J. F.; Bisri, S. Z.; Derenskyi, V.; Fritsch, M.; Fröhlich, N.; Allard, S.; Gordiichuk, P.; Herrmann, A.; et al. Semiconducting Single-Walled Carbon Nanotubes on Demand by Polymer Wrapping. *Adv. Mater.* **2013**, *25* (21), 2948–2956.

(32) Samanta, S. K.; Fritsch, M.; Scherf, U.; Gomulya, W.; Bisri, S. Z.; Loi, M. A. Conjugated Polymer-Assisted Dispersion of Single-Wall Carbon Nanotubes: The Power of Polymer Wrapping. *Acc. Chem. Res.* **2014**, *47* (8), 2446–2456.

(33) Nehls, B. S.; Asawapirom, U.; Füldner, S.; Preis, E.; Farrell, T.; Scherf, U. Semiconducting Polymers via Microwave-Assisted Suzuki and Stille Cross-Coupling Reactions. *Adv. Funct. Mater.* **2004**, *14* (4), 352–356.

(34) Greenham, N. C.; Samuel, I. D. W.; Hayes, G. R.; Phillips, R. T.; Kessener, Y. A. R. R.; Moratti, S. C.; Holmes, A. B.; Friend, R. H. Measurement of Absolute Photoluminescence Quantum Efficiencies in Conjugated Polymers. *Chemical Physics Letters*. 1995, pp 89–96.

(35) Koynov, K.; Bahtiar, A.; Ahn, T.; Cordeiro, R. M.; Hörhold, H. H.; Bubeck, C. Molecular Weight Dependence of Chain Orientation and Optical Constants of Thin Films of the Conjugated Polymer MEH-PPV. *Macromolecules* **2006**, *39* (25), 8692–8698.

(36) Kim, H.; Byun, Y.; Das, R. R.; Choi, B.-K.; Ahn, P.-S. Small Molecule Based and Solution Processed Highly Efficient Red Electrophosphorescent Organic Light Emitting Devices. *Appl. Phys. Lett.* **2007**, *91* (9), 093512.

(37) Lee, T. W.; Noh, T.; Shin, H. W.; Kwon, O.; Park, J. J.; Choi, B. K.; Kim, M. S.; Shin, D. W.; Kim, Y. R. Characteristics of Solution-Processed Small-Molecule Organic Films and Light-Emitting Diodes Compared with Their Vacuum-Deposited Counterparts. *Adv. Funct. Mater.* **2009**, *19* (10), 1625–1630.

(38) Kwak, G.; Lee, W. E.; Jeong, H.; Sakaguchi, T.; Fujiki, M. Swelling-Induced Emission Enhancement in Substituted Acetylene Polymer Film with Large Fractional Free Volume: Fluorescence Response to Organic Solvent Stimuli. *Macromolecules* **2009**, *42* (1), 20–24.

(39) Mitchell, W. J.; Burn, P. L.; Thomas, R. K.; Fragneto, G.; Markham, J. P. J.; Samuel, I. D. W. Relating the Physical Structure and Optical Properties of Conjugated Polymers Using Neutron Reflectivity in Combination with Photoluminescence Spectroscopy. *J. Appl. Phys.* **2004**, *95* (5), 2391–2396.

Table of Contents Image:

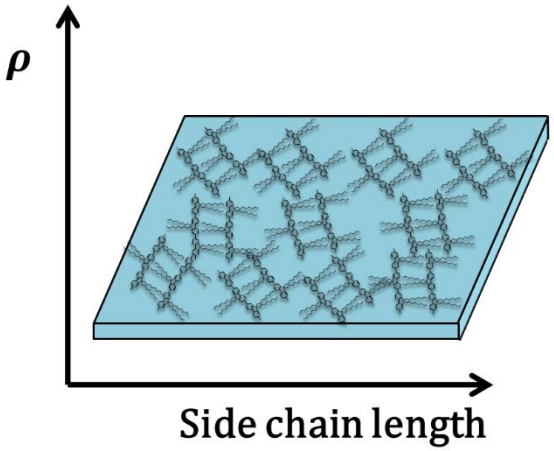

Material	Molecular weight of molecules or repeat unit of polymer [g/mol]
T3 butyl	3167
T3 hexyl	3840
T3 octyl	4513
PF8	389
PF12	501
PF15	585

Table 1. Molecular weights of the truxenes molecules and of the polyfluorene polymer repeat units

Material	Peak absorption wavelength [nm]	PL peak wavelengths [nm]	PLQY [%]
PF 8	386	423, 445	36
PF12	392	432, 456	54
PF15	395	422, 446	40
T3butyl	364	413, 437	63
T3hexl	367	412, 435	83
T3octyl	368	412, 435	80

Table 2. PLQY and peak wavelengths of the thin films absorption and PL spectra of polyfluorenes and oligofluorene truxenes

Material	Density [g/cm^3]	Volume / Molecule [nm^3]	Mean spacing (1D) [nm]
T3 butyl	0.90	5.84	1.8
T3 hexyl	0.87	7.33	1.94
T3 octyl	0.84	8.92	2.07

Table 3. Average molecular volume and molecular spacing of the truxene molecules in thin films

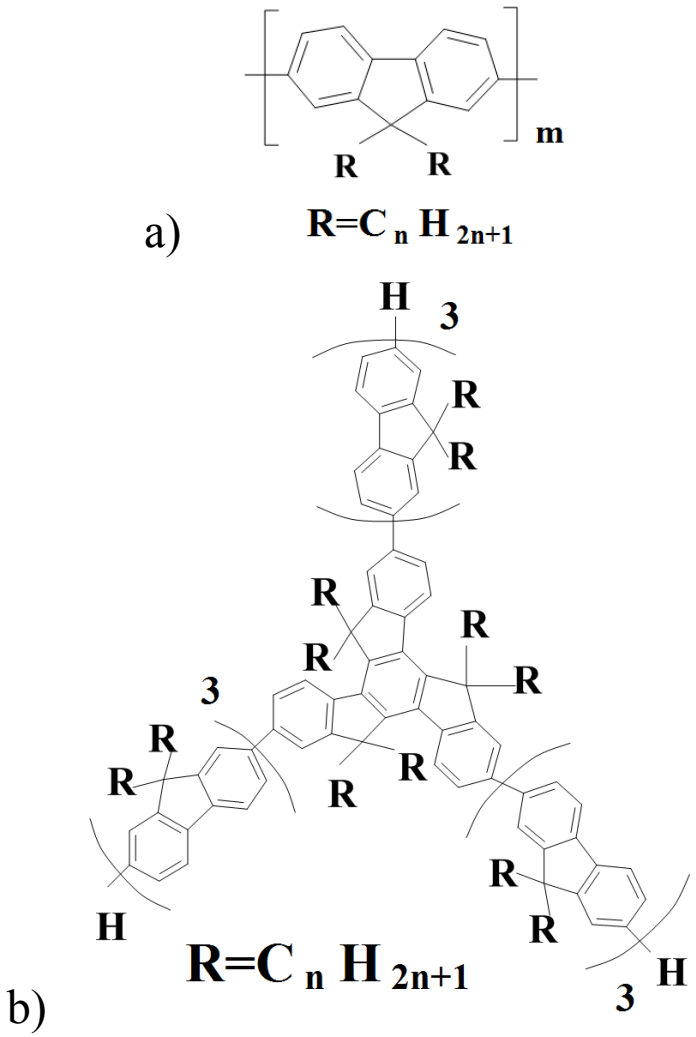

Figure 1. Chemical structure of the molecules used in the studies. 1a) di-alkyl polyfluorene, where the side chains consist of n=8, 12, or 15 carbon atoms; 1b) tris(terfluorenyl)truxene, where the side chains consist of n = 4, 6, or 8 carbon atoms

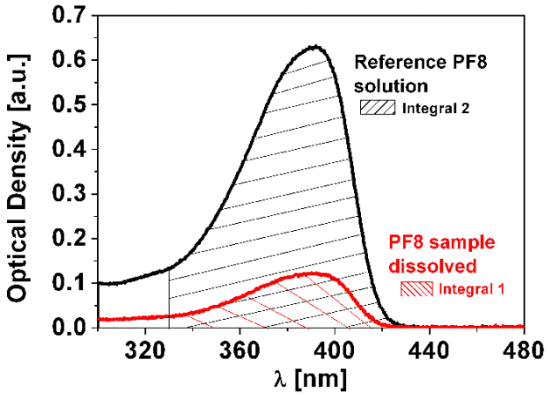

Figure 2. Absorption spectra of a PF8 sample dissolved in 3 ml of solvent and PF8 reference solution. The integral under the absorbance curve was used to calculate the mass of the polymer film.

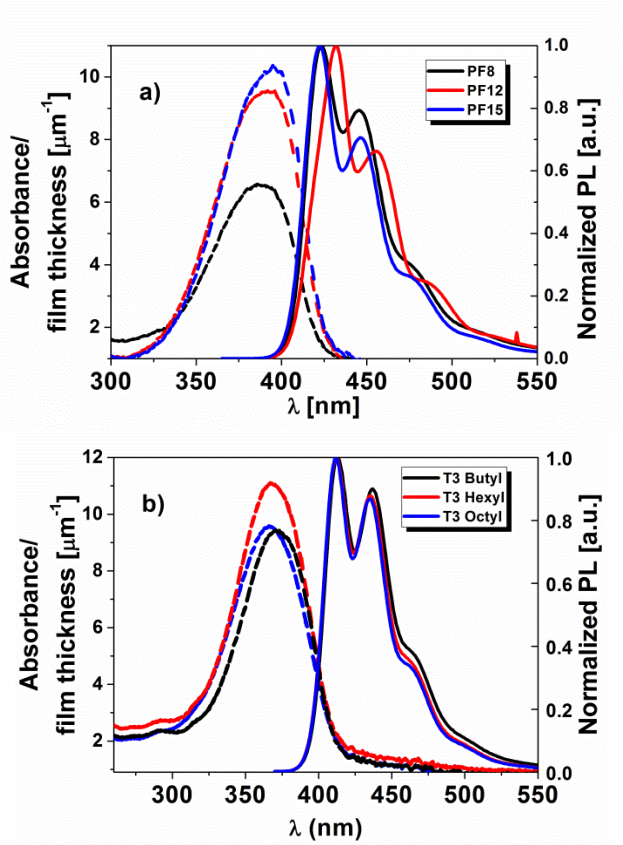

Figure 3a) Absorption (dashed line) and fluorescence (solid line) spectra of the polyfluorene films. Figure 3b) Absorption and fluorescence spectra of truxene films.

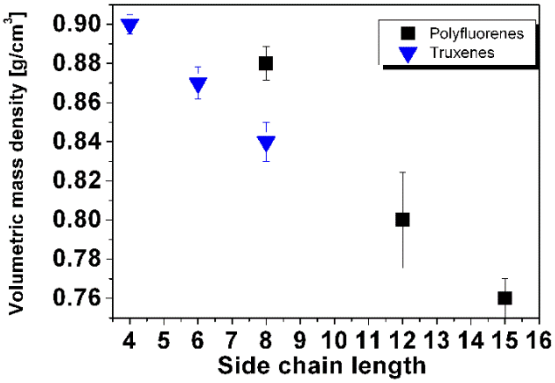

Figure 4. Mass density obtained for polyfluorenes (black squares) and truxenes (blue triangles) as a function of the number of carbon atoms in the alkyl side chains.

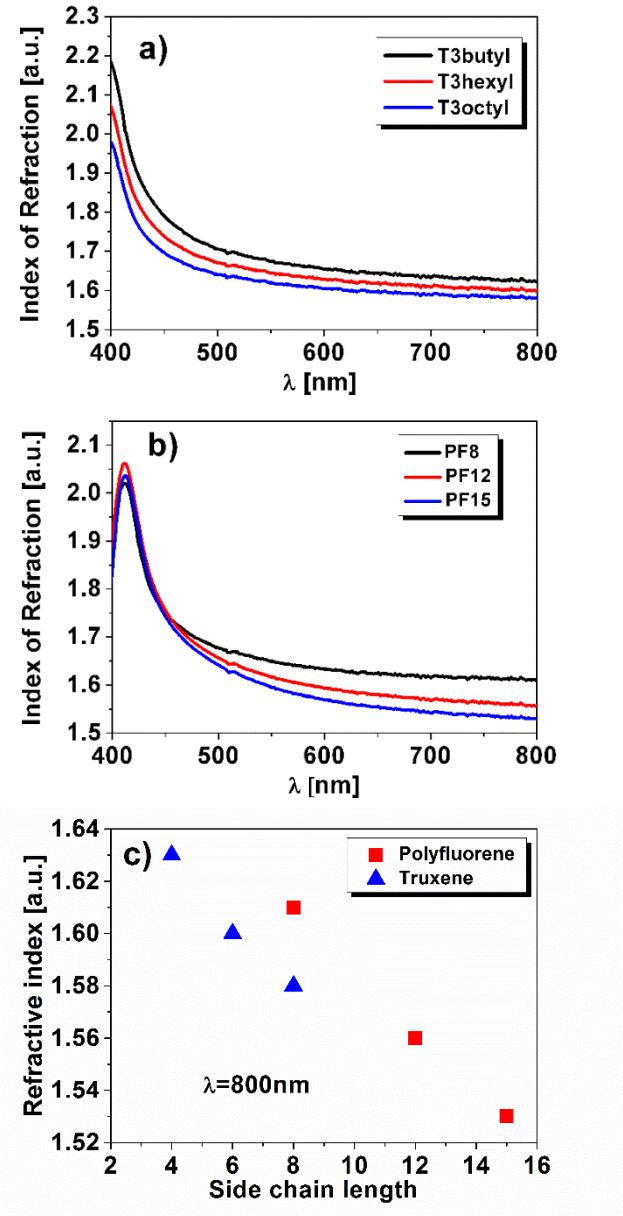

Figure 5 a) the refractive index measured by spectroscopic ellipsometry of the oligofluorene truxenes; b) the refractive index of polyfluorenes; c) the refractive index dependence on side chain length for truxene molecules and polyfluorenes, measured at a wavelength of 800 nm.